

## Resonant Self-Focusing of Laser Light in a Plasma

Chan Joshi, Christopher E. Clayton, and Francis F. Chen

*University of California, Los Angeles, California 90024*

(Received 19 January 1982)

When laser light containing two frequencies  $\omega_1$  and  $\omega_2$  impinges on a plasma with  $\omega_p = \omega_1 - \omega_2$ , plasma waves are resonantly excited. The ponderomotive force of these waves is much larger than that of the beam, and the self-focusing effect is greatly enhanced. With use of CO<sub>2</sub> laser light of only  $5 \times 10^9$  W/cm<sup>2</sup> intensity and a plasma at 0.6% of critical density  $n_c$ , this effect is observed as a strong ( $10^5$ -fold) enhancement of refracted light at  $\theta = 5^\circ - 12^\circ$  when the density is at the resonant value.

PACS numbers: 52.35.Mw, 52.25.Ps, 42.65.Cq, 52.40.Db

In laser-driven inertial-confinement fusion, the use of multiline lasers has been suggested as a means of suppressing undesirable parametric instabilities such as stimulated Brillouin scattering. Though a broadband pump has been shown<sup>1</sup> to be helpful, use of a discrete-line spectrum incurs a risk that other instabilities may be driven at resonant layers where the plasma frequency  $\omega_p$  matches the frequency difference  $\Delta\omega$  between two lines. In particular, we suggest a sequence of events in which optical mixing first excites a plasma wave, which is driven to larger amplitude by stimulated Raman scattering in the forward direction; the ponderomotive force  $F_{NL}$  of the plasma wave then creates a density depression on axis, causing a deflection of the laser beam by refraction. Such a mechanism could alter the focusing of beams onto a small target. The effect is similar to ponderomotive self-focusing of light by a plasma, but the plasma wave greatly amplifies the effect because of its larger ponderomotive force.

The standard theory of self-focusing has been applied to plasmas by Max,<sup>2</sup> and we use an extension of Ref. 2 to explain the observations. Assume a locally Gaussian beam profile and make the paraxial ray approximation. The amplitude of the light wave ( $\omega_0, k_0$ ) is then given by

$$E(z) = (E_0/f) \exp(-r^2/a^2 f^2), \quad (1)$$

where  $f(z)$ , the beam width factor, is determined by<sup>2</sup>

$$df/dz = -[R_0^{-2} + 2U(1) - 2U(f)]^{1/2} \quad (2)$$

with

$$U(f) = \frac{2}{k_0^2 a^4 f^2} + \frac{\exp(-\eta^2/f^2)}{k_0^2 a^2 \delta^2}. \quad (3)$$

Here  $a$  is the beam radius where it enters the plasma ( $z=0, f=1$ );  $\delta$  is the collisionless skin depth  $c/\omega_p$  calculated with the undisturbed den-

sity;  $R_0 = (-df/dz)_0^{-1}$  is the incident wave-front curvature radius; and

$$\eta = \eta_i = v_0/2v_i, \quad v_i^2 = (KT_e + KT_i)/m, \quad (4)$$

$v_0$  being the peak quiver velocity. At intensities below a critical value,<sup>2</sup>  $f$  will decrease from unity to  $f_{\min}$  at the focus and then increase indefinitely; at higher intensities the beam will oscillate in width. The turnaround at  $f_{\min}$  is the result of diffraction in the near-vacuum conditions created by  $F_{NL}$  near the focus; hence, it is essential to keep the exponential nonlinearity in Eq. (3). In the absence of plasma ( $\delta \rightarrow \infty$ ), Eq. (2) can be integrated to give the focal distance

$$z_0 = R_0(1 + 4R_0^2/k_0^2 a^4)^{-1}. \quad (5)$$

In a homogeneous plasma slab, Eq. (2) must be integrated numerically to give a new focal distance  $z_1$ . Applying this to an inhomogeneous plasma of dimension  $R$ , one can expect refraction to have a significant effect on the collimation of the exit beam when the focal shift  $\Delta z = z_0 - z_1$  is comparable to  $R$ .

To extend this formulation to resonant self-focusing, one merely has to replace  $E_0^2$  by an equivalent intensity  $AE_0^2$  due to the plasma wave, which is assumed also to have a Gaussian profile. The amplification factor  $A$  is found from the ponderomotive forces  $F_{NL}$  in each case:

$$F_{NL}(\text{light}) = -(\omega_p^2/\omega_0^2)\nabla\langle E_0^2\rangle/8\pi, \quad (6)$$

$$F_{NL}(\text{plasmon}) = -\nabla\langle E_p^2\rangle/8\pi, \quad (7)$$

where  $E_p$  is the amplitude of the plasma wave. Poisson's equation gives  $|E_p| = 4\pi en_1/k_p$ ; and, since  $|v_0| = eE_0/m\omega_0$  and  $v_\phi = \omega_p/k_p \approx c$  in forward Raman scattering, Eqs. (6) and (7) yield

$$A = \frac{F_{NL}(\text{plasmon})}{F_{NL}(\text{light})} = \frac{v_\phi n_1}{v_0 n_0} \approx \left(\frac{n_1/n_0}{v_0/c}\right)^2. \quad (8)$$

Since  $A$  can be very large (for instance,  $A = 122$

for  $n_1/n_0 = 1\%$  and  $I_0 = 10^{10}$  W/cm<sup>2</sup> of 10.6- $\mu$ m light), we neglect  $F_{NL}$  (light) in the presence of  $F_{NL}$  (plasmon); Eqs. (4) and (8) then give

$$\eta = \eta_p = (c/2v_t)(n_1/n_0). \quad (9)$$

As long as the plasma-wave amplitude has the same radial variation as the beam intensity, Eqs. (2) and (3) describe resonant self-focusing if Eq. (9) is used for  $\eta$  instead of Eq. (4).

The observations leading to the above analysis were made on a previously described setup<sup>3</sup> comprising a gain-switched 30-J CO<sub>2</sub> laser system and an arc plasma target in 4 Torr of argon. The radially incident laser beam is focused by an  $f/7.5$  lens to a 300- $\mu$ m-diam spot on the column axis. The undeflected beam, of half-angle  $\theta = 4^\circ$ , is blocked by a beam dump subtending  $\theta = 5^\circ$ . Forward-scattered radiation between  $\theta = 5^\circ$  and  $12^\circ$ , integrated over azimuth, is collected by an  $f/2$  lens, analyzed by an infrared monochromator, and detected by a Hg:Ge photoconductor. An intracavity SF<sub>6</sub> cell is used to produce various intensities of the 10.6- $\mu$ m (*P*-20), 9.55- $\mu$ m (*P*-20), and 10.26- $\mu$ m (*R*-16, 18, 20) lines. At a pressure of 3.5 Torr in the cell, the line ratio is approximately 0:1:1. Though we show data only

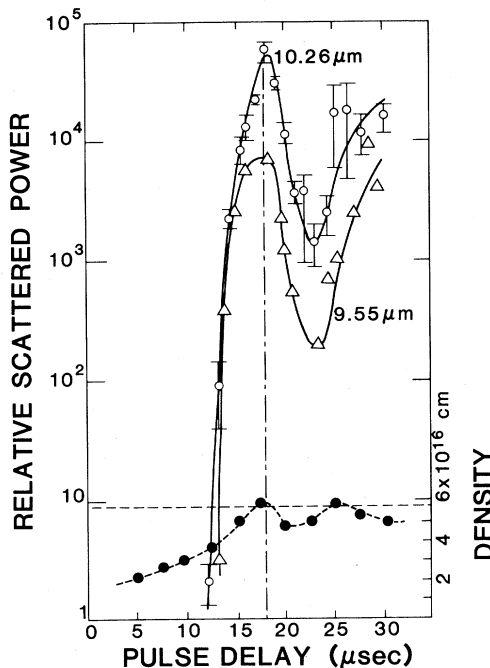


FIG. 1. Forward-scattered light (solid lines) and plasma density (dashed lines) as functions of pulse timing. The stray-light level is 1, and the 9.55- $\mu$ m data have been displaced one decade downwards for clarity.

for this case, the same saturation level was observed for a ratio as low as 0:1:10<sup>-2</sup>.

Figure 1 shows the dramatic change in forward-scattered light as the density is changed by varying the timing between the arc and the laser; the peak signal is almost 10<sup>5</sup> times the stray-light level. It is seen that the effect occurs whenever the density is close to  $n_r = 5.8 \times 10^{16}$  cm<sup>-3</sup>, at which  $\omega_p$  equals the beat frequency  $\Delta\omega$  between the 9.55- and 10.26- $\mu$ m lines. The density resonance is shown unambiguously in Fig. 2, in spite of a small systematic error between two methods of measuring the density. Uniformity of the density along the laser axis is shown in Fig. 3, obtained by Abel inversion of a ruby-laser interferogram. Figure 4 shows the dependence on incident intensity at  $n = n_r$ . Threshold is below  $6 \times 10^8$  W/cm<sup>2</sup>, and saturation is reached at  $2 \times 10^{10}$  W/cm<sup>2</sup>. The falloff at high  $I_0$  is due to a (measured) rise in  $n$  from  $6 \times 10^{16}$  to  $8 \times 10^{16}$  cm<sup>-3</sup> resulting from laser heating and ionization. This

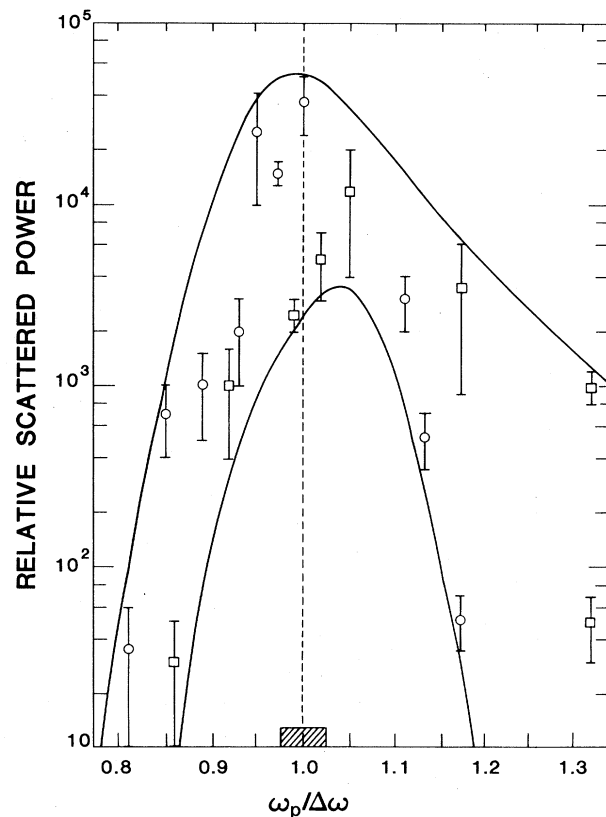


FIG. 2. Forward-scattered light in the 10.3- $\mu$ m line vs  $\omega_p/\Delta\omega$ , with density measured by ruby interferometry (squares) and by Stark broadening of a seed gas H $\alpha$  line. The shaded area indicates the spread of difference frequencies in the incident beam.

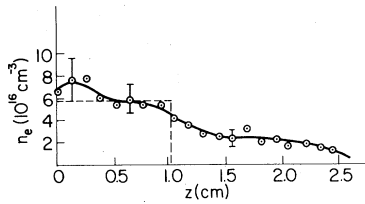


FIG. 3. Plasma density profile along the laser axis.

effect also shortens the scattered light pulse at high powers.

By varying the line intensity ratio and, particularly, by using a weak, nonresonant 10.6- $\mu\text{m}$  probe line, it was determined that the scattered light had no measurable frequency shift ( $<3$  GHz). The light is refracted and *not* red- or blue-shifted by an amount  $\omega_p$ . Yet the density resonance requires the existence of a plasma wave  $\omega_p$ . Direct detection of this wave by ruby Thomson scattering is impossible because of the large value of  $\alpha = 1/k\lambda_D$ . An attempt to detect a Stark-excited forbidden line<sup>4</sup> of a He seed gas failed. However, evidence of the plasma wave was found in a line around 11  $\mu\text{m}$  (Fig. 4, inset), which is presumably the beat between  $\omega_p$  and the 10.26- $\mu\text{m}$  line. The 11- $\mu\text{m}$  line is  $30\times$  stray light and appears only at  $n = n_r$ .

To compare with theory, we take  $R_0 \approx 1$  cm, approximately the radius of the uniform plasma. The  $f$  number of 7.5 then implies  $a = \frac{1}{7.5}$  cm. For our arc conditions  $T_e = 5$  eV and  $T_i \approx T_e/3$ , we have  $\eta_i^2 = 1.57 \times 10^{-12} I_0$  for 10- $\mu\text{m}$  light. A density of  $5.8 \times 10^{16} \text{ cm}^{-3}$  gives  $\delta = 22.1 \mu\text{m}$ . Numerical solution of Eq. (2) for these parameters yields the curves  $f(z)$  shown in Fig. 5 for various values of  $\eta^2$ . These curves show an increasing focus shift up to  $\eta^2 = \frac{1}{2}$ ; for higher  $\eta$ , the focusing returns to its vacuum state as the ponderomotive force blows the plasma out of the beam. The inset of Fig. 5 shows the focus shift  $\Delta z$  vs  $\eta^2$  and the corresponding values of  $I_0$  (if  $\eta = \eta_i$ ) and  $n_1/n_0$  (if  $\eta = \eta_p$ ). It is seen that ordinary self-focusing would not be observable at intensities of  $\approx 10^9 \text{ W/cm}^2$  without the resonance amplification effect.

Saturation of the plasma wave would occur at  $n_1/n_0 = 1$  if it were caused by wave breaking ( $\bar{v}_e \approx v_\phi$ ). Pressure balance, however, sets a much lower limit. Setting  $F_{NL}$  (plasmon) equal to  $dp/dr$ , we find  $n_1/n_0 = 2v_i/c \approx 0.7\%$  at  $T_e = 5$  eV. Actually, Fig. 5 (inset) shows that the refraction effect saturates at a lower value; the peak of  $\Delta z$  occurs at  $\eta^2 = 0.3$ , corresponding to  $n_1/n_0 = 0.4\%$ . This level is consistent with that ( $\approx 1\%$ ) inferred from the

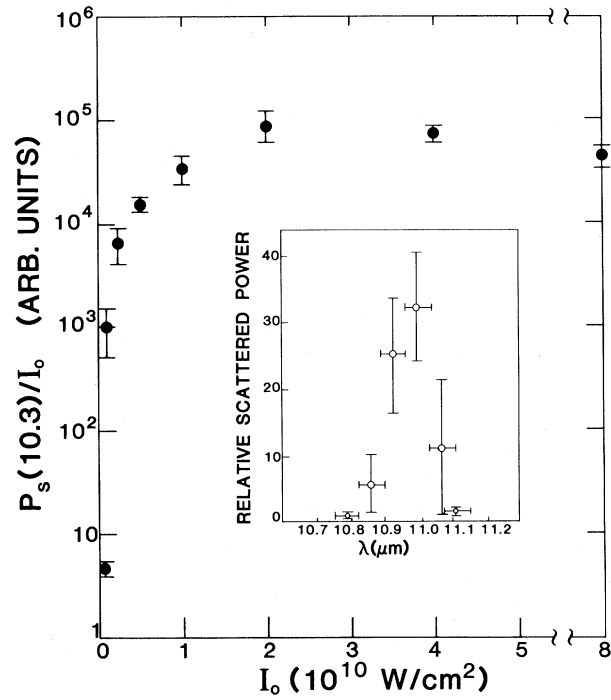


FIG. 4. Growth curve of forward-scattered light. The maximum ratio  $P_s/I_0$  corresponds to a refracted power of 25%. Inset: Spectrum of satellite observed near 11.0  $\mu\text{m}$ .

intensity of the 11- $\mu\text{m}$  line assuming that it is produced by Thomson scattering of 10.26- $\mu\text{m}$  light by the plasma wave.

We must now relate  $n_1/n_0$  to the pump intensity

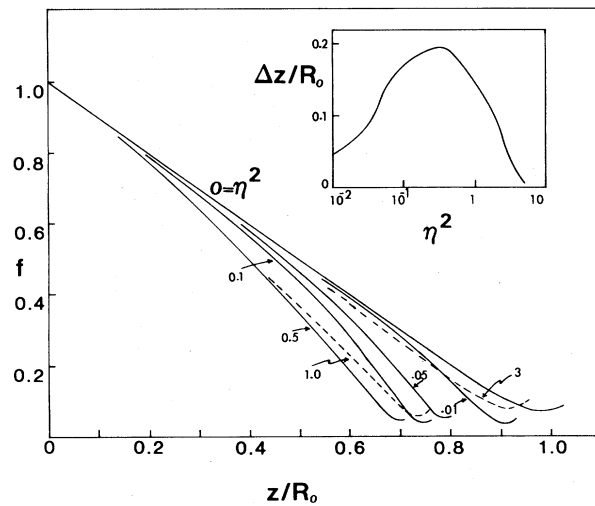


FIG. 5. Relative beam radius  $f$  vs distance  $z$  for various ponderomotive force parameters  $\eta^2$ . Inset: The focus shift  $\Delta z$  vs  $\eta^2$ .

$I_0$ . When the pump lines are equally strong, no stimulated Raman growth is necessary; and we may use optical mixing theory. In a homogeneous plasma, relativistic nonlinearity of the wave limits its amplitude to<sup>5</sup>

$$\frac{n_1}{n_0} = \left( \frac{16}{3} \frac{v_{01}}{c} \frac{v_{02}}{c} \right)^{1/3} = \left( \frac{8}{3} \frac{v_0^2}{c^2} \right)^{1/3} \approx 6 \times 10^{-6} I_0^{1/3}. \quad (10)$$

In a finite plasma, convection limits the wave amplitude. The group velocity is  $v_g = 3v_e^2/v_\phi \approx 3v_e^2/c$ , and the radial distance is  $af_{\min}$ , where  $f_{\min} \approx 0.04$  from Fig. 5. The wave energy  $W = E_p^2/8\pi$  is thus lost at the rate  $dW/dt = Wv_g/af_{\min}$ . The wave amplitude  $\xi$  grows linearly with time<sup>5</sup>:

$$\xi = \tilde{v}_e/\omega_p = (v_{01}v_{02}/c^2)\omega_p t/4k_p \approx (v_0^2/8c^2)ct.$$

The wave gains energy  $W \propto \xi^2$  at the rate  $dW/dt = 2W/t$ , which equals the loss rate at  $t = 2L/v_g$ , when the amplitude is

$$\frac{n_1}{n_0} = \frac{v_0^2}{v_e^2} \frac{\omega_p af_{\min}}{12c} \approx 8.5 \times 10^{-13} I_0. \quad (11)$$

Thus convection is the limiting factor for  $I_0 < 1.9 \times 10^{10}$ , and we use Eq. (11). Setting  $n_1/n_0 = 0.4\%$  in Eq. (11), we find that  $I_0 = 4.6 \times 10^9$  W/cm<sup>2</sup> at

saturation, in reasonable agreement with Fig. 4.

The threshold may be defined as the intensity where  $A = 1$ . From Eqs. (8) and (11), we find a threshold intensity  $I_0 = 1.1 \times 10^8$  W/cm<sup>2</sup>, again in reasonable agreement with observations.

Resonant self-focusing is relevant both to laser fusion, where it is important to avoid density resonances by suitable profile modification, and to ionospheric experiments, where enhanced self-focusing can be used greatly to amplify microwave beam intensities.

Professor A. Yasuda collaborated in the measurements. This work was supported by the U. S. Department of Energy under Contract No. DE-AS08-81DP40135 and the National Science Foundation under Grant No. ECS80-03558.

<sup>1</sup>S. P. Obenschain, N. C. Luhmann, Jr., and P. T. Greiling, Phys. Rev. Lett. **36**, 1309 (1976).

<sup>2</sup>C. E. Max, Phys. Fluids **19**, 74 (1976).

<sup>3</sup>M. J. Herbst, C. E. Clayton, W. A. Peebles, and F. F. Chen, Phys. Fluids **23**, 1319 (1980).

<sup>4</sup>J. J. Turechek and F. F. Chen, Phys. Fluids **24**, 1126 (1981).

<sup>5</sup>M. N. Rosenbluth and C. S. Liu, Phys. Rev. Lett. **29**, 701 (1972).